Available online at www.sciencedirect.com
ScienceDirect
Journal of Photochemistry and Photobiology A: Chemistry 192 (2007) 41–48
Journal of Photochemistry and Photobiology A:Chemistry
www.elsevier.com/locate/jphotochem

Photochemistry of the pesticide azinphos methyl and its model molecule 1,2,3-benzotriazin-4(3*H*)-one in aqueous solutions: Kinetic and analytical studies

Matthieu Ménager, Xijun Pan, Pascal Wong-Wah-Chung, Mohamed Sarakha *

Laboratoire de Photochimie Moléculaire et Macromoléculaire, UMR CNRS 6505, Université Blaise Pascal, F-63177 Aubière-Cedex, France

Received 7 March 2007; received in revised form 27 April 2007; accepted 1 May 2007
Available online 5 May 2007

Abstract

The photodegradation of the organophosphorus pesticide azinphos methyl and 1,2,3-benzotriazin-4(3*H*)-one in aqueous solutions with excitation within the wavelength range 254–313 nm was studied. For both compounds, the degradation depended on the excitation wavelength: the quantum yield decreased with decreasing the excitation energy.

The analysis of the irradiated solution of azinphos methyl revealed the presence of several products. 1,2,3-Benzotriazin-4(3*H*)-one was shown to be the major product accounting for roughly 50% of azinphos methyl conversion. Such product led in its turn to an efficient formation of anthralinic acid via the formation of an iminoketene derivative. Detailed mechanisms for the formation of the primary products from both azinphos methyl and 1,2,3-benzotriazin-4(3*H*)-one are proposed and discussed.

Keywords: Organophosphorus; Azinphos methyl; Photolysis; 1,2,3-Benzotriazin-4(3*H*)-one; Iminoketene; Anthranilic acid

1. Introduction

The presence of persistent organic chemicals in groundwater, streams, rivers lakes and waste water effluents may cause serious problems to the environment, human health and to the equilibrium of ecosystems. Among these pollutants, the pesticides represent an important class. The interest in these environmental effects leads to an increase of the research activities toward the development of new treatment methods which could help in an efficient remediation of contaminated waters. Many of these pollutants which are present in aqueous solutions can undergo photochemical transformation with solar light via direct as well as indirect photoreactions. Several pesticides present absorption spectra with an important overlap with that of solar light emission ($\lambda > 295$ nm). They can therefore undergo direct photochemical dissociation in the environment [1–4] permitting the formation of various byproducts. If the pesticide does not absorb the solar light, they may still undergo photochemical transfomation via indirect photoreaction. It is therefore of interest to know to what extent they are degraded via such interesting and low cost processes.

Azinphos methyl (*O*,*O*-diethyl *S*-[(4-oxo-1,2,3-benzotriazin-3(4*H*)-yl) methyl] ester is an insecticide from organophosphorus family which has been used as an alternative to organochlorine compounds for pest control. Such chemicals are included in several lists of pollutants due to their widespread use and high toxicity [5,6]. They have relatively high solubilities in water thus they are transported readily through soils and into ground waters or surfaces waters [5]. Several studies on the degradation of various organophosphorus compounds were undertaken such as photoassisted titanium dioxide mediated degradation [7,8], electrogenerated Fenton's reagent [9], Photo Fenton reaction [10], biodegradation [11], X-ray irradiation [12] and combined degradation using both semiconductors and organic sensitizers [13]. Azinphos methyl is widely and efficienly used to protect apple, peaches, lemon trees and fruits from a variety of insects. Its application on numerous agricultural and vegetable crops, fruits and vegetables is tolerated in several countries [14].

Recent studies on the degradation of azinphos methyl reported the formation of several products, identified using

* Corresponding author. Tel.: +33 4 73 40 71 70; fax: +33 4 73 40 77 00.
E-mail address: Mohamed.SARAKHA@univ-bpclermont.fr (M. Sarakha).

1010-6030/$ – see front matter © 2007 Elsevier B.V. All rights reserved.
doi:10.1016/j.jphotochem.2007.05.001

GC–MS analysis [15]. It was clearly reported that the photodecomposition mainly involves the dissociation of the C–S and the N–C bonds. The triazinic products, A and D, are known pollutants present in the environment due to their use as herbicides [16–18]. Within this work, the toxicity measurements of the irradiated solution of azinphos methyl by using acethylcholine esterase thermal lens spectrometer bioassay (AChE-TLS) [19] revealed a 30% decrease of initial AChE activity. Since AChE was not susceptible to the inhibition byproducts E and A, the detected reduced activity of the enzyme was mainly attributed to the formation of the trimethyl phosphate esters B and C but it could also be owing to non detected or secondary photoproducts.

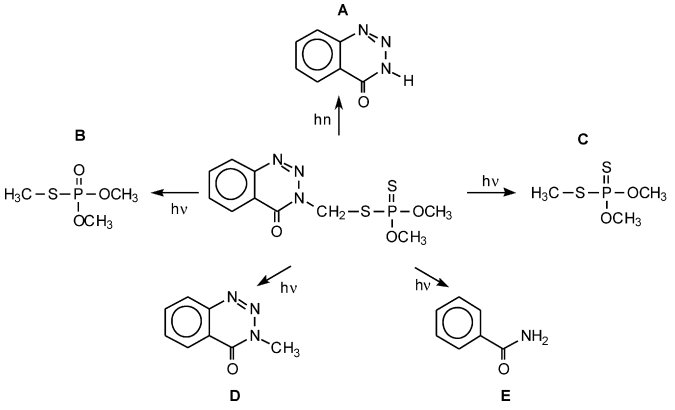

The photodecomposition of azinphos methyl was also shown to occur efficiently on soils and leaf surfaces [20]. The rate of disappearance increased with increasing soil moisture content. From analytical point of view, the noninsecticidal water-soluble photoproducts due to sunlight excitation amounted to roughly 1.4–6.5%. They were identified as to *N*-methylbenzazimide (D), 1,2,3-benzotriazin-4(3*H*)-one (A) and the oxon derivative of azinphos methyl.

The present study was conducted in order to get a better insight into the photochemical behaviour of azinphos methyl. The specific objective is to elucidate the nature of the main photoproducts formed under UV irradiation which could be important in relation to their persistence in the environment and also to determine the conditions of their formation. The kinetic aspect of azinphos methyl photodegradation is also of great importance in order to elucidate the mechanism of the formation of these products during the irradiation process using both conventional and time resolving techniques.

2. Experimental

2.1. Materials

Azinphos methyl (*O*,*O*-diethyl *S*-[(4-oxo-1,2,3-benzotriazin-3(4*H*)-yl) methyl] ester was purchased from Riedel-de Haën (98.5%). 1,2,3-Benzotriazin-4(3*H*)-one was from Aldrich (98%). Antranilic acid was provided by Fluka (>99.5%). They were all used as received. All other reactants were of the highest grade available. All solutions were prepared with deionised ultrapure water which was purified with Milli-Q device (Millipore) and its purity was controlled by its resistivity.

The following abbreviations were used throughout all the text:

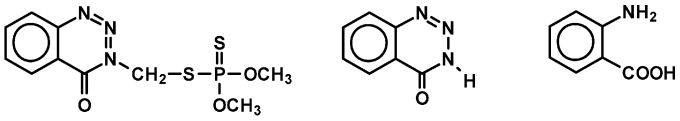

Azinphos-methyl **AZM** | 1,2,3 benzotriazin-4(3H)-one **BZT** | Anthranilic acid **ACA**

2.2. Steady state irradiations

For kinetic as well as analytical purposes, aqueous solutions were irradiated with a parallel beam using a xenon arc lamp (1600 W) equipped with a Schoeffel monochromator. The bandwidth was 10 nm. Solution in a quartz cell (1 cm optical pathlength) was deoxygenated by argon or nitrogen bubbling or oxygenated by oxygen bubbling for 20 min prior to irradiation. Then the cell was closed using a septum. The initial concentration of the solution was checked by HPLC analysis after bubbling. The irradiations at 254 nm were obtained with PHILIPS TUV 6 W lamp delivering a parallel beam. Potassium ferrioxalate was used as a chemical actinometer as reported in the literature [21]. The pH of the solutions was adjusted using dilute solutions of $HClO_4$ or NaOH. For analytical purposes, irradiations were performed in a device equipped with germicide lamps (up to 6) emitting at 254 nm and a 100 ml cylindrical quartz reactor. Similar setup was used for the irradiation at 313 nm. The deaeration of the solution was accomplished by continuous nitrogen bubbling.

2.3. Laser flash photolysis

Transient absorption experiments in the 20 ns to 400 μs time scale were carried out on a nanosecond laser flash photolysis spectrometer from Applied Photophysics (LKS.60). Excitation (λ = 266 nm) was from the fourth harmonic of a Quanta Ray GCR 130-01 Nd:YAG laser (pulse width ≈5 ns), and was used in a right-angle geometry with respect to the monitoring light beam. A 3 cm^3 volume of an argon saturated solution was used in a quartz cell, and was stirred after each flash irradiation. Individual cell samples were used for a maximum of five consecutive experiments. The transient absorbance at preselected wavelength was monitored by a detection system consisting of a pulsed xenon lamp (150 W), monochromator, and a 1P28 photomultiplier. A spectrometer control unit was used for synchronizing the pulsed light source and programmable shutters with the laser output. This also housed the high-voltage power supply for the photomultiplier. The signal from the photomultiplier was digitized by a programmable digital oscilloscope (HP54522A). A 32 bits RISC-processor kinetic spectrometer workstation was used to analyse the digitized signal.

2.4. Analyses

UV–vis spectra were recorded on a Cary 300 scan (Varian) spectrophotometer LC/MS studies were carried out with

Q-TOF-Micro/water 2699 from CRMP center at the University Blaise Pascal. It is equipped with an electrospray ionisation source (ESI) and a Waters photodiode array detector. Each single experiment permitted the simultaneous recording of both UV chromatogram at a preselected wavelength and an ESI-MS full scan. Data acquisition and processing were performed by MassLynx NT 3.5 system. Chromatography was run using a Nucleosil column100-5 C18 ec (250 mm × 4.6 mm, 5 μm). Samples (5–10 μl) were injected either directly or after evaporation of the solvent for better detection. The following gradient program was used by employing water with 0.4% acetic acid (A) and acetonitrile (B) at 1 ml min^{-1}.

Time (min)	Initial	3	13	20	30
%A	95	80	80	5	95
%B	5	20	20	95	5

The consumption of azinphos methyl and the formation of the byproducts were monitored by analytical HPLC using a HP1050 apparatus equipped with a photodiode array detector. The experiments were performed by UV detection at either 228 or 280 nm and by using a reverse phase Macherey Nagel column (Nucleodur C8, 250 mm × 4.6 mm, 5 μm). The flow rate was 1.0 ml min^{-1} and the injected volume was 50 μL. The elution was accomplished with acidified water (acetic acid 0.4%) and acetonitrile in isocratic mode (1/1 by volume). pH measurements were carried out with a JENWAY 3310 pH-meter equipped with an Ag/AgCl glass combination electrode 9102 Orion. The pH of the solutions was adjusted using dilute solutions of HCl or NaOH. The accuracy achieved was within ±0.01 pH units.

3. Results

3.1. Kinetics

The stationary UV spectrum of azinphos methyl (AZM) in aqueous solution displays a weak absorption band with a maximum at 284 nm and showing a well identified vibrational structure which is attributed to the presence of the triazine moiety. The molar extinction coefficient was evaluated to 6800 $mol^{-1}\,l\,cm^{-1}$. It also shows a strong absorption band at 226 nm (27,900 $mol^{-1}\,l\,cm^{-1}$) corresponding to the π–π* transition. Under our experimental conditions, No changes were observed within the pH range 1.5–9. The absorption is very significant at λ > 300 nm indicating that AZM is able to absorb solar light and thus to undergo direct photochemical reactions. It is worth noting that no degradation occurred when a solution of the insecticide was left in the dark for several hours.

As shown in Fig. 1, the 254 nm irradiation of aerated solution at pH 5.5 of AZM (3.3×10^{-5} mol l^{-1}) led to important changes on the absorption spectrum. The absorbance decreased within the wavelength range 220–325 nm which reflects the photodecomposition of AZM, whereas it increased at shorter and longer wavelengths owing to the formation of byproducts. Moreover, the first absorption band showed an important shift from 284 to 276 nm during the course of irradiation more likely due to the formation of a final product. The HPLC analysis clearly showed

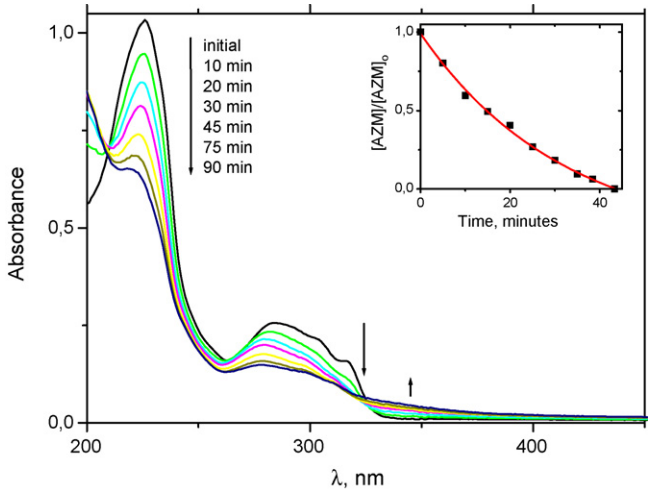

Fig. 1. UV–vis absorption changes observed for the irradiation of aerated solution of azinphos methyl AZM (3.3×10^{-5} mol l^{-1}) upon excitation at 254 nm at pH 5.5. The insert shows the disappearance of AZM obtained by HPLC measurements as a function of irradiation time.

that AZM efficiently disappeared within 40 min irradiation time under our experimental conditions (see insert Fig. 1).

It is worth noting that similar changes on the absorption spectrum as a function of irradiation time and also similar degradation kinetic profile were observed by excitation within the wavelength region 254–310 nm using a xenon lamp setup. For excitation at longer wavelengths, e.g. 300 nm, the complete disappearance occurred after a much longer irradiation time. This is due to the low absorbance but also to an excitation wavelength effect phenomenon as will be reported hereafter.

The quantum yield of azinphos methyl disappearance was measured in various experimental conditions. The data are reported in Table 1.

In deoxygenated aqueous solutions at pH 5.5, the quantum yield of disappearance was evaluated to 2.1×10^{-2} when the excitation wavelength was set to 254 nm. The efficiency of the photochemical reaction was found to increase by increasing oxygen concentration. Moreover, the excitation at 313 nm led to a disappearance quantum yield seven times lower than that obtained at 254 nm. Such excitation wavelength effect was further demonstrated by performing the experiments within the excitation wavelength range 254–313 nm. As clearly shown in Fig. 2, the quantum yield decreased when the excitation energy increased. This is probably owing to the excitation of AZM in its second absorption band, namely the π–π* band. Such effect has been reported with several organophosphorus compounds in aqueous solutions [22]. It is worth to note that all the attempts

Table 1
Effect of the excitation wavelength and oxygen concentration on azinphos methyl disappearance quantum yield

λ_{exc} (nm)	Deoxygenated $[O_2] < 10^{-5}$ mol l^{-1}	Air saturated $[O_2] = 2.7 \times 10^{-4}$ mol l^{-1}	Oxygen saturated $[O_2] = 1.27 \times 10^{-3}$ mol l^{-1}
254	2.1×10^{-2}	3.1×10^{-2}	4.9×10^{-2}
313	3.3×10^{-3}	4.2×10^{-3}	6.5×10^{-3}

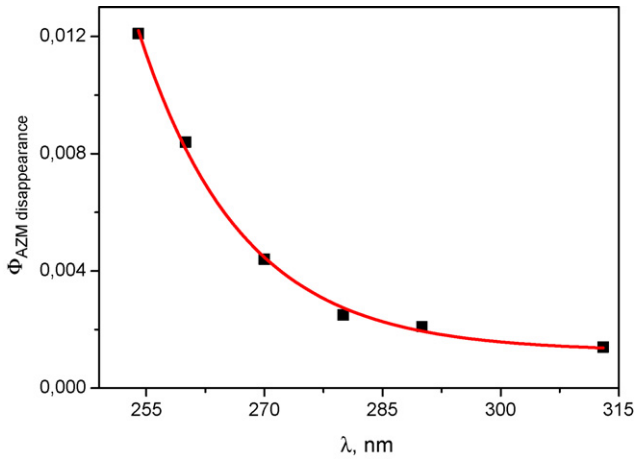

Fig. 2. The evolution of the azinphos methyl disappearance quantum yield as a function of excitation wavelength in air saturated solution and at pH 5.5.

to detect significant transient species absorbance by nanosecond laser flash photolysis at 266 nm failed.

3.2. Analytical studies

The identification of the byproducts formed by azinphos methyl photodegradation was made using LC/ESI/MS measurements. Fig. 3 depicts the UV chromatogram recorded at 228 nm. It was obtained for a solution of AZM (3.8×10^{-5} mol l^{-1}) irradiated in a cylindrical reactor emitting at 313 nm in air saturated conditions and at pH of 5.5.

It clearly shows the presence of several photoproducts which are eluted before azinphos methyl ($t_{ret} = 12.0$ min) indicating that we are dealing with smaller and/or more polar products when compared to the parent compound. Among them, P1 ($t_{ret} = 3.7$ min) and P3 ($t_{ret} = 4.3$ min) were clearly major products and accumulate in the solution. The LC/ESI/MS data are reported in Table 2. Under our experimental conditions, the experiments were mainly realized in ES positive mode which

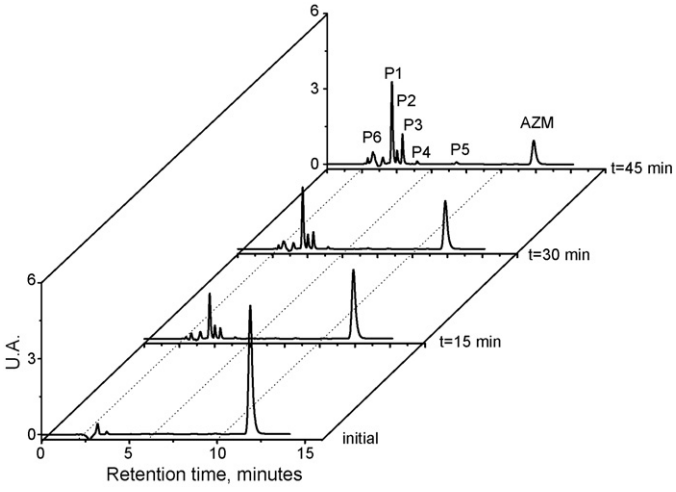

Fig. 3. HPLC chromatograms ($\lambda_{detection} = 228$ nm) as a function of irradiation time obtained for the irradiation of AZM (3.3×10^{-5} mol l^{-1}) in air saturated aqueous solution at pH 5.5 and at $\lambda_{excitation} = 313$ nm.

Table 2
The main fragment ions obtained for BZT and ACA in the LC/ESI/MS

Structures	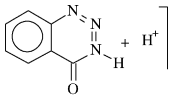 m/z =148	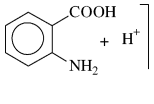 m/z=138
Main common fragment ions	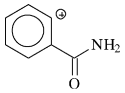 m/z=120	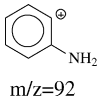 m/z=92

appeared to be more sensitive and suitable for the parent compound as well as for the majority of photogenerated products. P1 ($[M+H]^+ = 148$) was easily identified as 1,2,3-benzotriazin-4(3*H*)-one (BZT). The structures of the identified fragments ($m/z = 120$ and $m/z = 92$) are reported in Table 2.

The absorption spectrum of BZT displays a weak absorption band with a maximum at 276 nm and showing a vibrational structure, similar to that observed with AZM, as well as a strong absorption band at 226 nm. The position of the former absorption band undoubtedly explains the shift observed on Fig. 1 and fits well with those of the spectrum obtained after the complete disappearance of azinphos methyl (Fig. 1). Since BZT was commercially available, it was possible to quantify its formation and thus to determine its formation quantum yield which was evaluated to 0.016 at 254 nm, showing that it represents 50% of azinphos methyl conversion. As observed with AZM, the BZT disappearance quantum yield showed a dependence on the excitation wavelength leading us to the conclusion that such effect could be due to the presence of the triazine structure. It should be noted that the formation of BZT through the irradiation of AZM was observed in small amount when the experiment were performed in pure acetonitrile solutions.

P3 ($[M+H]^+ = 148$) was identified as anthranilic acid (ACA). As shown in Table 2, it ESI mass spectrum led to the same fragmentation ions as BZT. Its UV spectrum showed three well defined absorption maxima without any detectable vibrational structure indicating the loss of the triazine moiety: 219, 248 and 330 nm.

The formation kinetic profiles of both products, namely BZT and ACA, showed that the former is a primary product while the latter is more likely arising from secondary reactions via BZT (Fig. 4). This hypothesis will be discussed in the following sections

Some other products were also detected by LC/MS and the proposed structures are as follows:

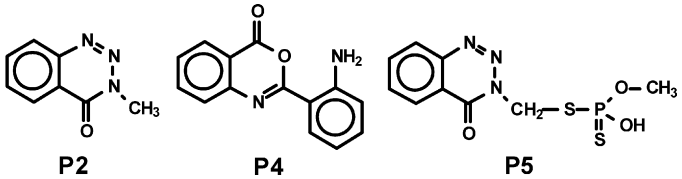

All the observed byproducts were formed when the excitation was performed within the range 254–313 showing once again a similar photochemical behaviour whatever the excitation

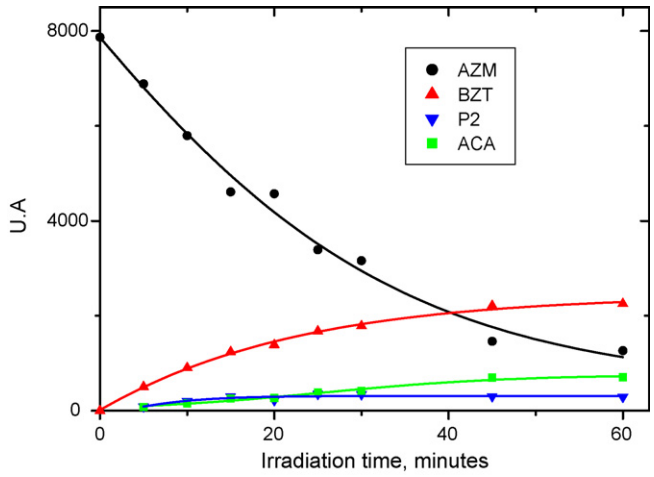

Fig. 4. The evolution of AZM concentration and byproduct formation as a function of irradiation time in air saturated solution. [AZM] = 3.3×10^{-5} mol l^{-1}, pH 5.5, $\lambda_{excitation}$ = 254 nm.

wavelength. The LC/MS in ESI negative mode experiments also permitted the detection of small molecules such as *O*,*O*-dimethyl hydrogen dithiophosphate (P6), its oxon derivative (P7), phosphorodithioic *O*,*O*,*S*-trimethyl ester (P8) and phosphorothioic *O*,*O*,*S*-trimethyl ester (P9).

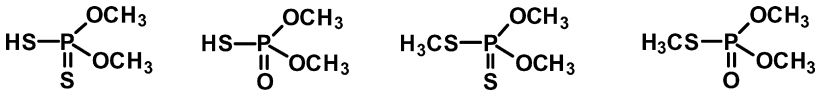

It is worth noting that the oxon derivative arising from an oxidative process of AZM was not detected under our experimental conditions. Such oxidative reaction was efficiently observed with several organophophorus compounds [15,23]. The lack in the detection of oxon product is more likely owing to its efficient photodegradation.

The quantum yield of BZT formation, the main primary byproduct, was evaluated to 1.3×10^{-2} in aerated solution indicating that it accounts for 50% of BZM conversion.

Since BZT represents the major byproduct and also to elucidate the formation mechanism of the secondary byproducts, we undertook in detail the study of the photochemical behaviour of BZT in aqueous solutions.

3.3. Photochemical behaviour of 1,2,3-benzotriazin-4(3H)-one (BZT)

The absorption spectrum of BZT at pH 5.5 showed two well defined bands at 280 nm (8800 mol^{-1} l cm^{-1}) and 225 nm (32,000 mol^{-1} l cm^{-1}). The former was red shifted when the pH of the solution increased due to a protolytic equilibrium. The anionic form presented an absorption band at 301 nm (15,600 mol^{-1} l cm^{-1}). The pK_a, obtained by studying the changes of the absorbance at 280 nm as a function of pH, was evaluated to 7.8. No degradation was observed when a solution of BZT was left in the dark for several hours.

Aqueous solutions of BZT (1.2×10^{-5} mol l^{-1}) in aerated conditions were irradiated at 254 nm solution at pH 5.5. The spectrophotometric changes were monitored by taking the UV–vis spectra at regular time intervals. The resulting spectra show the decrease of the band at 276 nm without any sign of shift and the increase of the absorbance around 330 nm (Fig. 5a). Similar spectral changes were observed by excitation within the range 254–320 nm but the rate of disappearance decreasing by increasing the excitation wavelength.

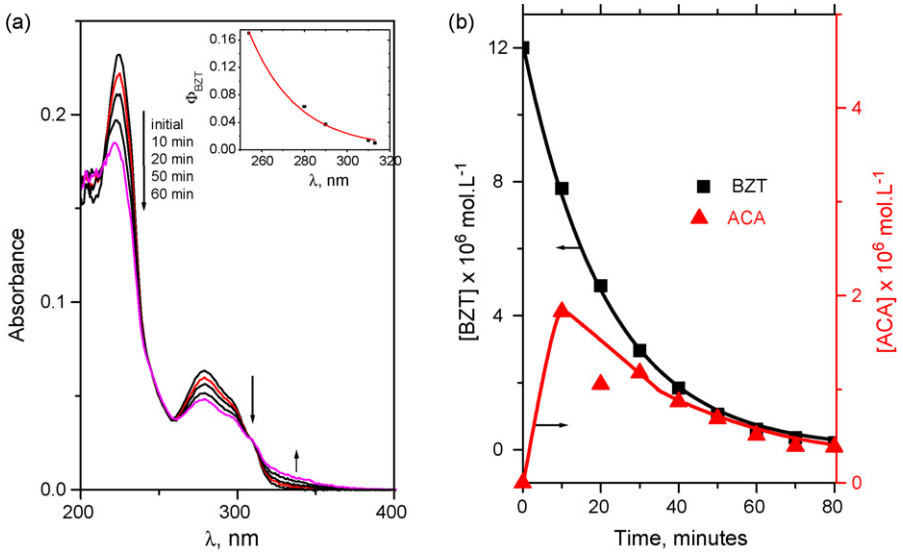

Fig. 5. (**a**) UV–vis absorption changes observed for the irradiation of aerated solution of 1,2,3-benzotriazin-4(3*H*)-one (**BZT**) (1.2×10^{-5} mol l^{-1}) upon excitation at 254 nm at pH 5.5. (**b**) The disappearance of BZT and the formation of anthranilic acid as a function of irradiation time.

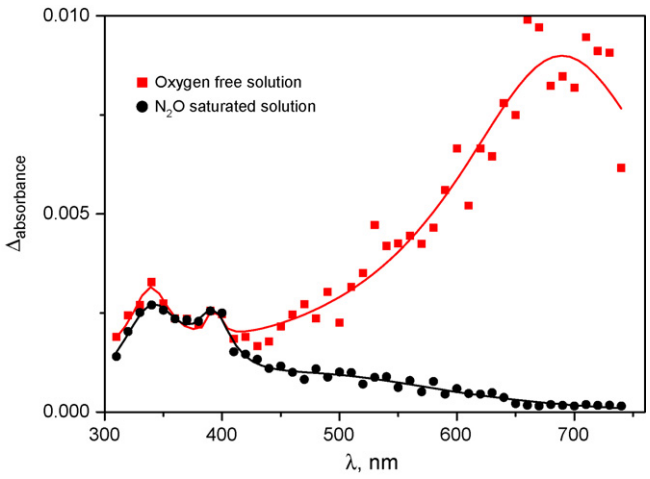

Fig. 6. Transient absorption spectra obtained after the pulse of a oxygen-free aqueous solution of azinphos methyl (4.0×10^{-5} mol^{-1} l s^{-1}, pH 5.5, $\lambda_{excitation} = 266$ nm).

The disappearance quantum yield was evaluated to 7.0×10^{-3} in air saturated conditions and at pH 5.5. It significantly increased when the experiments were performed in oxygen free solutions ($\Phi = 17.0 \times 10^{-3}$) and also at pH > 7 showing that the anionic form is more photoreactive and that the oxygen partially inhibited the process.

It is important to note that the quantum yield of BZT disappearance showed a dependence on the excitation energy similar to that observed with azinphos methyl (see insert Fig. 5a). It was evaluated to 1.0×10^{-3} at 313 nm.

In order to have a better insight into the transformation mechanism scheme, we undertook nanosecond laser flash photolysis experiments. The laser excitation from the fourth harmonic (266 nm) of Nd:YAG laser of an argon saturated aqueous solution of BZT led to the development of absorption bands within the whole wavelength region 280–800 nm (Fig. 6). At the end of the laser pulse, three different absorption bands were clearly observed: 340, 390 and 720 nm. The decay profiles at these wavelengths showed that two intermediate species were formed. The first one absorbs at 340 and 390 nm and the second one at 720 nm. The latter species was easily assigned to the solvated electron species. It rapidly disappeared in the presence of molecular oxygen and N_2O used as electron scavenger [24]. Its amount of formation as monitored by its initial absorption was linearly dependent upon the initial light intensity within the 1–10 mJ laser energy range, showing that we are dealing with a monophotonic process. The second transient, namely that absorbing at 340 and 390 nm, was rapidly quenched by molecular oxygen with a second rate constant of 3.9×10^9 mol^{-1} l s^{-1}. It is more likely assigned to the triplet state of BZT.

The LC/MS analysis of an irradiated solution showed that anthranilic acid ACA (P3) was present as the major product together with a small amount of P3. The absorption spectrum of anthranilic acid which presents three absorption bands: 335, 245 and 220 nm, perfectly explains the increase of the absorbance at λ > 320 nm observed in Fig. 5a. Its formation as a function of irradiation time showed that it is more likely a primary product representing more than 50% of BZT conversion but it disappeared photochemically in its turn for prolonged irradiation time (Fig. 5b). It is worth noting that when the irradiation of BZT was undertaken in pure acetonitrile solution, anthranilic acid was formed in trace concentration. The changes on the absorption spectrum as a function of irradiation time showed the development of a new band with a maximum at 340 nm corresponding to the accumulation of P4 in the solution.

4. Discussion and mechanism

As clearly shown from the kinetic studies, the disappearance of both azinphos methyl (AZM) and 1,2,3-benzotriazin-4(3*H*)-one (BZT) appears to be efficient at the excitation into the higher energy absorption band, namely π–π* band. Such effect has been observed with several organophosphorus compounds but was not clearly explained [22]. In the case of AZM and BTZ, this could be due to a photoionisation process or to the involvement of various excited states. Moreover, the homolytic dissociation of the N–N bonds in the triazine part can not be completely ruled out. Such bond scission, which can occur at short wavelength, will lead to the cleavage of the triazine moiety. On the contrary to the case of BZT, the disappearance of the organophosphorus AZM does not significantly involve the triplet excited state.

From the kinetic and analytical studies, the main photodegradation process lead to the formation of 1,2,3-benzotriazin-4(3*H*)-one (BZT) which accounts for roughly 50% of the conversion. Since its amount decreased when the experiment was performed in pure acetonitrile solution, BZT may be the result of a photohydrolysis reaction through the singlet excited state. According to the literature [25], the obtained phosphorus part is further hydrolyzed permitting the formation of *O*,*O*-dimethyl hydrogen dithiophosphate (P6) as proposed below:

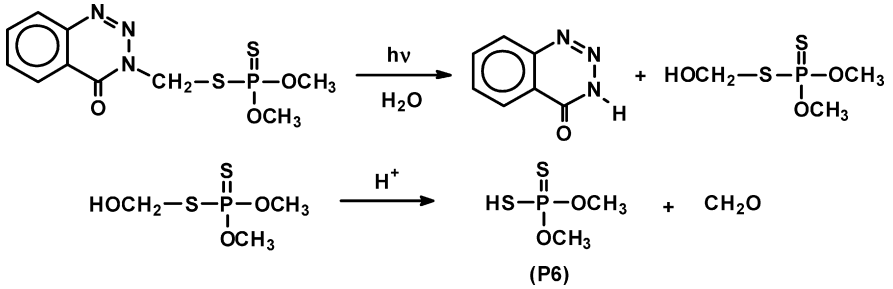

The possible reaction of water molecules with various AZM excited states is in favour with the effect of the excitation wavelength on BZT formation.

Several homolytic dissociations can be suggested for the photochemical formation of products BZT, P2, P4, P6 and P8. They involve the homolytic scission either of the N–C bond, C–S bond or P–O bond. The presence of hydrogen donor molecules (RH) such as the starting pesticide or any byproducts is necessary for achieving the process as suggested by the following scheme:

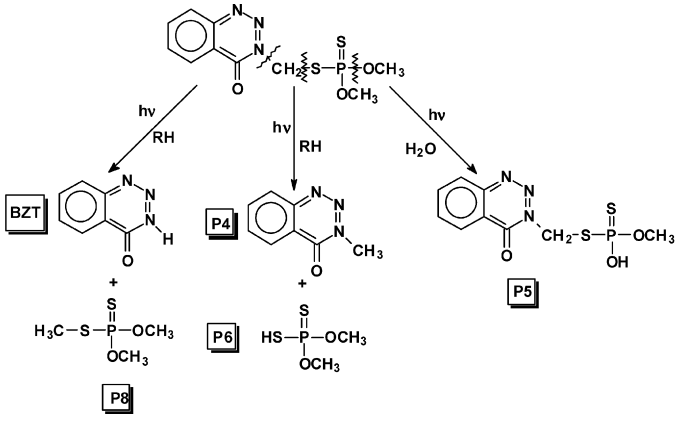

The absence of the oxon derivative under our experimental conditions is probably due to its rapid photochemical dissociation. The formation of P7 and P9 via either the hydrolysis or homolytic scission of N–C and C–S bonds in the oxon compound is in favor of this conclusion.

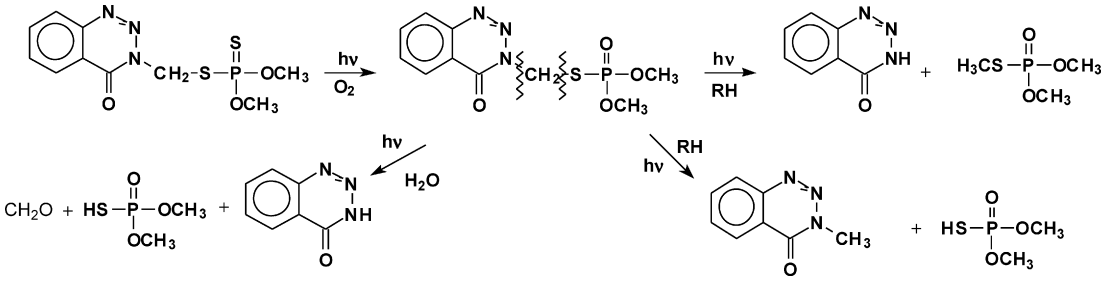

The formation kinetics of anthranilic acid is clearly showed the involvement of a secondary process which involves the photochemical behaviour of BZT through the triplet excited state as clearly demonstrated by laser flash photolysis. It could also arise from the homolytic dissociation of the N–N on the triazine group. The increase of the BZT quantum yield disappearance in the absence of oxygen reveals that the triplet excited state pathway represents the main degradation pathway. In both case, the intermediate formation of the iminoketene derivative (**I**) may take place. Such species was reported in the literature to be formed for the thermolysis and flash vacuum pyrolysis of either 1,2,3-benzotriazin-4(3*H*)-one (BZT) or isatoic anhydride [26–29]. This species may be in equilibrium with its isomer benzoazetinone (**II**) [29]. Under our experimental conditions, it was not possible to detect such species, most likely owing to the rapid hydrolysis process permitting the formation of the final product, anthranilic acid.

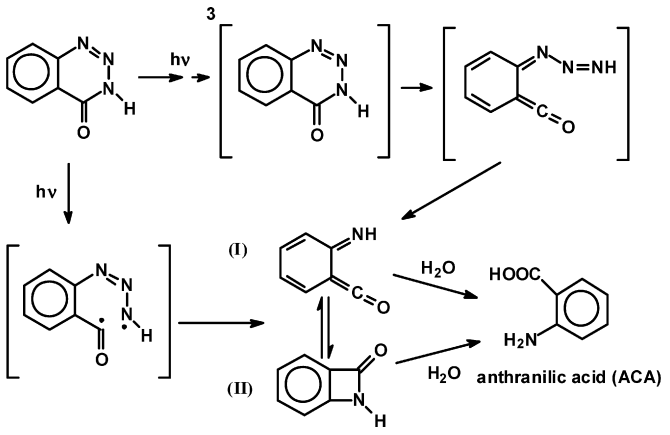

In the absence of water, the formation of anthranilic acid was inhibited in favour of P4 through a dimerisation process of the iminoketene intermediate as proposed while studying the thermolysis of 1,2,3-benzotriazin-4(3*H*)-one (BZT) [26,28]

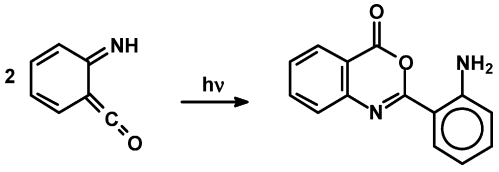

5. Conclusion

The photochemistry of the two compounds, the organophosphorus azinphos methyl (AZM) and its model molecule 1,2,3-benzotriazin-4(3*H*)-one (BZT), has been elucidated. In both cases, the disappearance quantum yield was found to be excitation wavelength dependent in the range 254–313 nm owing either to the involvement of various excited states or to the homolytic dissociation of the N–N bonds of the triazine structure of the molecule. Initial hydrolysis reaction leading to the cleavage of the N–C bond mainly leads to the formation of BZT. Several other byproducts arising from C–S or P–O bond scission were also formed. In the case of BZT, the photochemical process in aqueous solutions mainly led to anthranilic acid via the triplet state pathway and the formation of an iminoketene intermediate.

Acknowledgements

The authors would like to thank Bertrand Legeret, from the "Laboratoire Synthèse Et Etude de Systèmes à Intérêt

Biologique, SESSIB" for his kind and helpful assistance with the LC/MS/MS experiments.

References

[1] H.D. Burrows, L.M. Canle, J.A. Santabella, S. Steenken, J. Photochem. Photobiol. B: Biol. 67 (2002) 71–108, and references therein.
[2] O. Legrini, E. Oliveros, A.M. Braun, Chem. Rev. 93 (1993) 671.
[3] O. Hutzinger, Environmental Photochemistry, The Handbook of Environmental Chemistry, vol. 2, Springer, 1999, Part L and references therein.
[4] M.L. Canle, J.A. Santaballa, E. Vulliet, J. Photochem. Photobiol. A: Chem. 175 (2005) 192–200.
[5] V.K. Ragnarsdottir, Environmental fate and toxicology of organophosphate pesticides, J. Geol. Soc. Lond. 157 (2000) 859–876.
[6] G. Morchio, R. De Andreis, G.R. Verga, Riv. Ital. Sostanze Grasse 69 (1992) 147–157.
[7] R. Doong, W. Chang, J. Photochem. Photobiol. A: Chem. 107 (1997) 239–244.
[8] V.A. Sakkas, D.A. Lambropoulou, T.M. Sakellarides, T.A. Albanis, Anal. Chem. Acta 432 (2001) 59.
[9] E. Guivarch, N. Oturan, M.A. Oturan, Environ. Chem. Lett. 1 (2003) 165–168.
[10] P.L. Huston, J.J. Pignatello, Water Res. 33 (5) (1999) 1238–1246.
[11] K. Ohshiro, T. Kakuta, T. Sakai, H. Hirota, T. Hoshino, T. Uchiyama, J. Ferment. Bioeng. 82 (3) (1996) 299–305.
[12] P. Trebse, I. Arcon, Radiat. Phys. Chem. 67 (2003) 527–530.
[13] S.A. Naman, Z.A.-A. Khammas, F.M. Hussein, J. Photochem. Photobiol. A: Chem. 153 (2002) 229–236.
[14] C.G. Flocco, M.P. Carranza, L.G. Carvajal, R.M. Loewy, A.M. Pechen, A.M. Giulietti, STOTEN 327 (2004) 31–39.
[15] B. Bavcon Kralj, M. Franko, P. Trebse, Chemosphere 67 (2007) 99–107.
[16] J.C. Heidker, R.S. Pardini, Bull. Environ. Contam. Toxicol. 8 (3) (1972) 141–146.
[17] E.D. Woodland, G. Lawson, N. Ostah, J. Pharm. Pharmacol. 48 (2) (1996) 223–227.
[18] C.D.S. Tomlin (Ed.), British Crop Protection Council, Surrey, England, 1997, pp. 67–68.
[19] M. Franko, M. Sarakha, A. Cibej, A. Boskin, M. Bavcon, P. Trebse, Pure Appl. Chem. 77 (10) (2005) 1727–1736.
[20] T.T. Liang, E.P. Lichtenstein, J. Agric. Food Chem. 24 (6) (1976) 1205–1210.
[21] J.G. Calvert, J.M. Pitts, Photochemistry, Wiley, New York, 1996, pp. 783–786.
[22] H.B. Wan, M.K. Wong, C.Y. Mok, J. Agric. Food Chem. 42 (1994) 2625–2630.
[23] H. Floesser-Mueller, W. Schwack, Rev. Environ. Contam. Toxicol. 172 (2001) 129–228.
[24] G.V. Buxton, C.L. Greennstock, W.P. Helman, A.P. Ross, J. Phys. Chem. 17 (1988) 513–886.
[25] M. Sanchez-Camazano, M.J. Sanchez-Martin, Clays Clay Miner. 36 (6) (1991) 609–613.
[26] A.W. Murray, K. Vaughan, J. Chem. Soc. (1970) 2070–2074.
[27] H.E. Crabtree, R.K. Smalley, H. Suschitzky, J. Chem. Soc. (1968) 2730–2733.
[28] R.K. Smalley, H. Suschitzky, Tetrahedron Lett. 29 (1966) 3465–3469.
[29] S.-J. Chiu, C.-H. Chou, Tetrahedron Lett. 40 (1999) 9271–9272.